Journal of Energy Research and Reviews

12(1): 16-35, 2022; Article no.JENRR.89970
ISSN: 2581-8368

Central Composite Design of Biodiesel Production from Waste Cooking Oil using *Tympanotonus fuscatus (Periwinkle)* Shells as Catalyst

Ubani O. Amune [a*] and Shegun K. Otoikhian [a]

[a] Department of Chemical Engineering, Edo State University Uzairue, Iyamho-Uzairue, Edo State, Nigeria.

Authors' contributions

This work was carried out in collaboration between both authors. Author UOA conceptualization, methodology, software, validation, formal analysis, investigation, resources, data curation, writing both original draft and electronic draft of the manuscript. Author SKO formal analysis, investigation, resources, data curation, provide financial support, methodology, software, supervision of the manuscript. Both authors read and approved the final manuscript.

Article Information

DOI: 10.9734/JENRR/2022/v12i130290

Open Peer Review History:
This journal follows the Advanced Open Peer Review policy. Identity of the Reviewers, Editor(s) and additional Reviewers, peer review comments, different versions of the manuscript, comments of the editors, etc are available here: https://www.sdiarticle5.com/review-history/89970

Original Research Article

Received 20 May 2022
Accepted 25 July 2022
Published 04 August 2022

ABSTRACT

Biodiesel has been generally accepted as an environmentally – safer alternative to fossil based fuels. However, concerns of the cost of production, use of acid catalysts leading to corrosion, and recovery of homogenous catalyst remain. This study therefore seeks to optimize the transesterification process parameters in the conversion of waste cooking oil (WCO) using waste *Tympanotonus fuscatus* shell (WTFS). The catalysts were characterized using XRD, FTIR, and XRF. Temperatures ranging from 30°C to 90°C, catalyst loading from 1 to 10% by weight, and reaction durations from 30 to 180 minutes were examined for the transesterification technique. The physiochemical properties of the waste cooking oil revealed a high acid value (10.02mgKOH/g), kinematic viscosity of 13.30 mm^2/s, pour point, 156^oC, flash point of 104^oC, Calorific value of 34.78 MJ/kg, carbon content of 2.65% m/m, among other parameters while the GCMS analysis indicated the presence of C_{16} to C_{21}. The biodiesel however showed an acid value of 0.416 mgKOH/g, viscosity of 4.638 mm^2/s, pour point of 0.3^oC, flash point of 104^oC, calorific value of 40.17 MJ/kg, and carbon content of 0.019% m/m which were in agreement with the EU and American standards. The elemental composition and crystalline structure of the catalyst revealed a considerable

**Corresponding author: E-mail: ubani.amune@edouniversity.edu.ng;*

concentration of CaO, MgO, Al_2O_3, SiO_2, and other metal oxides. The CCD approach used to design the experiments was significant ($p < 0.0001$) and the biodiesel synthesis which resulted in a maximum yield of 91.70% was obtained with 5.5% WFTS, 105 minutes of reaction time, 65 ^oC, and a 1:7 oil–Methanol ratio. The operating parameters of temperature ($p < 0.0001$), catalyst load ($p = 0.00713$), and time ($p = 0.0288$) all had significant effects on biodiesel yield; however, temperature had a stronger influence than the other process variables. The ANOVA results showed that the factors were extremely significant while Fit statistics and model comparison revealed a coefficient of determination of 97.66%, with the predicted value of 84.68% and the adjusted value of 95.00%. The biodiesel produced met the biodiesel standards.

Keywords: Central composite design; heterogeneous catalysts; optimization; response surface method; waste cooking oil; Waste Tympanotonus Fuscatus Shell (WFTS).

1. INTRODUCTION

The depletion of fossil fuel reserves and growing concerns about global warming have not slowed the world's rising energy demand. Conversely, this demand has exacerbated the energy crisis coupled with the growing population and industrial revolution. Renewable energy including solar, wind, geothermal, hydro, and biomass energy sources has become the response to these concerns [1] due to their distinct degradability, economic, and efficient characteristics [2]. Utilizing renewable energy sources is one of the most environmentally friendly ways the energy sector is contributing to sustainable development [3]. Biofuels from biomass has garnered matchless attention among other renewables because of certain disadvantages such as energy storage, influence of seasons on energy generation, unavailability of land mass attributed to other renewables. Contrariwise, the majority of these qualities are innate to biofuels such as biodiesel, biogas, and bioethanol, and can be thought of as defining characteristics of the fuels themselves [2]. Biodiesel stands out among all of these biodegradable fuels as being the one that most closely resembles conventional diesel in terms of its physicochemical properties like low aromatic and sulphur content, high viscosity, low volatility, low calorific value, lubricity, high flash point and cetane content, and overall feedstock regenerability, which can guarantee particulate matter by 47%, hydrocarbon emission by 67% [4], and approximately 70–90% reduction in GHG emission [2], [4]–[9]. These properties make them useful in several automobiles including ships, cars, air planes, amongst others [9].

Biodiesel is produced from either the esterification or transesterification reaction (depending on the precursor) of triglycerides including edible and non-edible oils, fat, waste-oils, microalgae gotten from plants and animals [1], [2], [4], [9], [10]. This reaction is carried out in the presence of an alcohol and a suitable catalyst to produce esters and water or fatty acid alkyl esters and glycerol respectively. The use of non-edible oil sources like Jatropha oil, neem oil, and rubber seed oil, amongst others, micro algae, and waste cooking oil (WCO) has been considered an appealing option that has the potential to lower the cost of producing biodiesel while ameliorating the concerns of food shortages due to the use of edible oils as biodiesel feedstock [2], [8], [11-14]. Millions of tons of WCO are being generated yearly with about 1 million from Malaysia [15], and a total of about 16.5 million tons worldwide [3], [16-18]. These volumes which are being wasted by open disposal on plants and animals alike [19] can be collected and converted into biodiesel creating dual-faced solution: prevention of environmental degradation and alternative feedstock for the energy sector [1], [12], [19].

In general, catalysts can be categorised as homogenous or heterogeneous. Homogeneous base catalysts exhibit a high level of catalytic activity under mild reaction conditions (40 to 65°C at normal atmospheric pressure) [14], [20]. However, homogeneous catalysts are plagued by technical issues such as soap formation, reactor corrosion, difficult catalyst recovery, and the production of vast quantities of polluted water, which increase the overall cost and dangers of biodiesel production [21-23]. Due to their eco-friendly and recyclable catalytic activities, the use of bio-based heterogeneous catalysts in biodiesel production has received special consideration [23], [24]. Heterogeneous catalysis has the potential to mitigate the various difficulties encountered when using homogeneous catalysts to produce biodiesel from low-cost feedstock. Heterogeneous catalysts have a number of technical benefits,

including simple separation and purification of reaction products, low production cost, decreased reactor corrosion, high stability, and low sensitivity to free fatty acids and moisture contents [23], [25]. Many research communities are focused on developing novel heterogeneous catalysts that are stable, durable, and efficient under ambient conditions [26]. Several research has focused on the exploitation of waste materials as catalysts (wood [27], sugar cane bagasse and oil palm trunk [28], corn cub [10], fly ash [5], [28], [29], wheat bran [23], egg and coconut shells [25], [30], plantain [31] and banana [32] peels, bones [33], etc.), due to their abundance and low cost of catalysts preparation. Solid base catalysts have higher catalytic activity than solid acid catalysts [34]. Different solid-base catalysts used in transesterification include CaO, MgO, Al_2O_3, SiO_2 etc. [35], KF/Al_2O_3. These catalysts produce over 92% yield of biodiesel under optimum reaction conditions.

A large portion of Nigeria's 12 million tonnes of waste shells are *Tympanotonus fuscatus* (Periwinkle) shells [36]. After consuming the edible part, the shells become waste and litter trash dumps, residential areas, and even local markets, causing land and air pollution [37]. Decomposing waste shells produce an offensive stench, leach and weather heavy metals from the dump, and contaminate public water systems [36], [38]. Several shells from eggs [5,7], [11], [25], [28], [39,41] and a variety of snails [40], [42,48] have been used, however, there aren't many studies [22], [49], [50] in literature on the use of WTFS as a heterogeneous catalyst for biodiesel production.

In this research, the bio-catalytic (WTFS) synthesis of waste cooking oil (WCO) was investigated through a two-step esterification and transesterification reaction. The synthesized catalyst was characterized by XRD, XRF, and FT-IR for functional groups, elemental composition, and crystalline structure. The WCO was pre-treated and stored for consequent characterization. Optimized Trans-esterification reaction was then carried out using the central composite design (CCD) of experiments and the products obtained were subsequently characterized for their physicochemical properties, alongside their functional groups (FT-IR), and GC-MS to determine the effect of the catalyst on the WCO. The catalyst was synthesized as recommended for the great performance breakdown of hydrocarbon chains. The central composite design (CCD) is a tool for statistical optimization that is used to maximise the many different factors that are involved in the system. CCD is the optimization method that is advised to use CCD is recommended when there are more than two factors at play in the system and the optimal value lies in the middle of the factor ranges. To optimise the biodiesel synthesis process, reaction parameters such as WTFS catalyst loading (wt. percent), reaction temperature (^oC), and residence time (minutes), were considered while the Response Surface Methodology (RSM) of statistical optimization technique based on CCD was utilised.

This work is original for several reasons:

i) Designed and characterized a functional heterogeneous catalyst for biodiesel production from an agricultural waste i.e. *Tympanotonus fuscatus* shell, which is abundant in the entire Southern-Nigeria;
ii) Optimized catalyst preparation parameters including activation with sulphuric acid, temperature and duration;
iii) Adoption of WTFS catalyst to produce biodiesel from high free fatty acids waste cooking oil;
iv) Optimization of the biodiesel production conditions with a full factorial design of experiments in conjunction with response surface methodology via central composite design;

The optimally produced biodiesel was characterised in accordance with ASTM and European (EN14214) standards. The most important aspect of this research is unquestionably the investigation into the synthesis of a bio-based heterogeneous catalyst.

2. EXPERIMENTAL

In the following is a list, functionality, and description of the materials and methods used to carry out the preparation, characterization, and experiment.

2.1 Materials

2.1.1 WCO and WTFS

The waste cooking oil (WCO) was provided by a local restaurant (chicken republic) in Ugbowo area of Benin city, while the WTFS was collected from Uselu Market, all in Benin city area of Edo State, Nigeria. The WCO collected is filtered, to remove any impurity and suspended matter or particles. This was heated at 120^oC while stirred

continuously for 2 hours to remove possible water content. The pre-treated WCO was hereafter stored in a clean container. The WTFS collected was thoroughly washed with water for three days consecutively to remove the dirt and remnant periwinkle flesh within the shells. The WTFS was then dried in direct sunlight for 3days to reduce the foul smell.

2.1.2 Chemicals

Distilled water, 99.5% pure methanol, Concentrated Sulphuric acid (H_2SO_4), Ethanol, Benzene, Potassium Hydroxide (KOH), Hydrochloric acid (HCl), Acetic acid, Chloroform, Wijs reagent, Phenolphthalein, Sodium thiosulphate, Potassium Iodide (KI), starch solution indicator, ice block. They were all of analytical grade obtained from Ken Chemical Shop, Benin city, Nigeria, and needed no further purification.

2.2 Methods

2.2.1 Preparation of catalyst

The preliminary sun-dried WTFS was further dried in oven (U-Tech SSI-107) at an average of 120^{o}C for 24 hours to remove excess water [51] before calcining in the electric-powered furnace (MXBAOHENG YTH-2.5-10) at a temperature rate of 0.1^{o}C/second till 900^{o}C [52] and then left for an additional 2 hours to ensure complete oxidation and convert any carbonate to oxides and bring out the maximum amount of metallic oxides. The calcined WTFS was then cooled before subjecting to pulverization manually with the use of a mortar and pestle to obtain fine powder. This was repeated three (3) times with the use of a sieve of mesh size 45µm to ensure proper separation, homogeneity, and diffraction of powdered catalyst. To avoid the use of contaminated active oxides in the WTFS catalyst from exposure to atmospheric water, moisture and carbon dioxide thereby forming less active hydrates and inactive carbonates, the powdered WTFS was then re-calcined again at 900 ^{o}C for 1 hour before removal from furnace and storage in a sealed glass desiccator while the temperature dropped to room temperature.

2.2.2 Characterization of catalyst

The X-ray diffraction (XRD) of the WTFS derived catalyst was performed on a sample of WTFS using the Brucker's D2-PHASER benchtop X-ray powder diffractometer furnished with Cu-Kα (1.541874 Å) radiation source. The XR software was set to 40KV and 40mA while the scan interval was from 10^{o} to 90^{o} 2θ with a step size of 0.02. The XR patterns of Ca, Mg, Al and Si majorly amongst others were collected at the 2θ axis of the detector using the powder method in a scintillating diffractometer.

The elemental chemical compositions of the materials were analysed using the HORIBA's MESA-50K X-ray fluorescence spectroscopy (XRF) to determine the compounds present (CaO, MgO, Al_2O_3 and SiO_2). The functional groups were determined by Fourier transform infrared (FT-IR, Bio-Rad 3000 Excalibur series with wave number range from 400 to 3000 cm^{-1}).

2.2.3 Characterization of WCO and biodiesel

The characteristics of the WCO, and Biodiesel was determined by relevant techniques based on majorly on ASTM and European (EN14214) International standards. The relative density was determined using ASTM D4052, the Kinematic viscosity was determined using the ASTM D7042. The Acid Value was determined using the ASTM D974 testing standards, Peroxide value was determined as described by the ASTM D3703 method, ASTM-D1959-97 was used to determine the Iodine value, ASTM D94 was used for the saponification value. The Glycerol content, Ester value and Free Fatty Acid (FFA) were both gotten from the saponification value and acid vales respectively. Pour point was determined using the American Standards for Testing and Methods in ASTM-D97, Pensky-Martens equipment was used to determine the flashpoint (ASTM-D93), ASTM-D2500 for cloud point, ASTM-D4297 for calorific value, and ASTM-D1500 standards was used to determine the carbon content.

Gas Chromatography coupled with Mass Spectrophotometry (GC-MS) of Hewlett-Packard HP 7890 was used to analyse the chemical composition of produced biodiesel. 5% phenylmethypolysiloxane was used to form a thick-film coating on the capillary column working with a 5975-quadrupole detector. The temperature ranged from 50^{0}C to 290^{0}C at the rate of 5^{0}C per min for 10 min in full scan mode between m/z 33-533 using split-less injection function at 290^{0}C and solvent interval of 3 min. The obtained peaks based on their retention times were matched with standard compound peaks of NIST08s mass spectral data library.

2.3 Biodiesel Production

2.3.1 Esterification reaction

The transesterification of WCO was initially carried out with a 7:1 methanol – oil ratio, temperature of 60 ^{o}C, 5.5% WTFS catalyst loading for 180 ^{o}C [53]. This yielded 21.35% biodiesel with plenty of soap formation along with the large amount of water proving Canakci & Sanli [54] right. Hence, since the conversion of oil to biodiesel can only be carried out with FFA of less than 1% [55], it became necessary to first esterify the oil (500 g) with sulphuric acid (5 g) dissolved in methanol (24 g) for 1hour at 60oC [53], [55]. Canakci [54] & Thangaraj [55] posited that the most common way is to convert free fatty acids into FAME by esterification using sulphuric acids, p-toluene sulfonic acids, or alkyl benzene sulfonic acids.

The mixture was heated in a three-neck round bottom flask connected with a reflux condenser to avoid methanol losses and heated on a magnetic stirrer with a thermocouple installed to keep the temperature constant. After completion of the reaction, the mixture was poured in a separation funnel and left to cool and settle overnight into two layers. Water in the lower layer was removed while FAME and unreacted triglyceride was subjected to the other transesterification process. This esterification process reduced the FFA content from 5.03% to 1.02% before transesterification with WTFS catalyst was carried out.

2.3.2 Synthesis of biodiesel

The transesterification reaction made use of a recommended 7:1 methanol – oil ratio, while three factors were varied; temperature ranging from 30 ^{o}C to 90 ^{o}C, WTFS catalyst loading of 1 to 10%wt. and residence time ranging from 30minutes to 180minutes [53], [56]–[61]. The process began with was weighing a known amount of the pre-treated oil and heating in a three-necked batch reactor to its specified reaction temperature according to the central composite experimental design (CCD). The catalyst is the weighed and dissolved in methanol with its ration to oil being set to 7:1 constant as the minimum optimal ratio needed to achieve over 80% conversion [53]. At the end of the reaction, the reaction mixture was then transferred into the separation funnel and left overnight to allow the separation of catalyst, glycerol and biodiesel (in that order from bottom to top). The upper phase (biodiesel phase) was obtained and further purified using a high-speed centrifuge to remove any suspended catalyst or glycerol. The purified biodiesel was stored in a closed-tight vial to be used for biodiesel characterization using Agilent Technologies 7890B GC system –5977A MSD (GC-MS) and Perkin Elmer Spectrum TM 100 FT-IR spectroscopy. The conversion was calculated in percentage using Equation (1).

$$Biodiesel\ Yield\ (\%) = \frac{Weight\ of\ Biodiesel}{Weight\ of\ WCO} \times 100\% \quad (1)$$

2.3.3 Design of experiment for biodiesel production, ANOVA statistics, and optimization

Three factors were studied; the amount (in weight percent) of WTFS (1 – 10%wt. in relation to the acid), reaction temperature (30^{o}C – 90^{o}C) and reaction time (30 – 180 minutes). RSM was employed to analyse the operating conditions of the transesterification reaction to obtain a high conversion percent. The experimental design was carried out by the three chosen independent process variables at three levels. The software “Design Expert 8P” was used for designing and analysing the experimental data. The independent variables (factors) and their levels, real values as well as coded values are presented in Table 1 generating twenty (20) experimental runs all together.

The model equation was used to predict the optimum values and subsequently to elucidate the interaction between the factors. The quadratic equation model for predicting the optimal point was expressed according to Equations (1) below and the response (y) was determined to be the biodiesel yield [62].

Table 1. Experimental design for transesterification of WCO

Name	Unit	Low	High	- alpha	+ alpha
Temperature	^{o}C	42.16	77.84	30	90
Catalyst load	wt.%	2.82	8.18	1	10
Time	minutes	60.40	149.60	30	180

$$y = \beta_o + \sum_{i=1}^{k} \beta_i x_i + \sum_{i=1}^{k} \beta_{ii} x_i^2 + \sum_{i=1}^{k=1} \sum_{j=i+1}^{k} \beta_{ij} x_i x_j + \varepsilon \quad (2)$$

The analysis of variance (ANOVA), was the statistical tool used for analysis used to establish the influence of each variable on the response (biodiesel) yield. The statistical analysis further produced the predicted values which were compared and contrasted with the responses obtained. On the output-factors graph, the anticipated value was plotted against the responses to reveal the lines–of–best–fit, which demonstrated the relationship between the considered variables. The process was optimized by determining the and sum of squares and lack of fit test. Specifically, the df, f-value, p-value, coefficient of determination (R-square), and regression co-efficient (experimented and predicted R-square values) were examined to demonstrate the suitability of the model. Graphing a function with a multi-dimensional input (AB; AC; BC; ABC) and a one-dimensional output (biodiesel yield) necessitates the charting of points in three-dimensional space to examine the effect of interaction variables.

3. RESULTS AND DISCUSSION

3.1 Properties of WCO, Biodiesel

The GC–MS results (Fig. 1) for the characterization of WCO are outlined in Table 2. For comparison purposes, they are tabled together with the Biodiesel results (Table 5). WCO trans-esterified in the presence of WTFS produced biodiesel which fell within the biodiesel European standard (EN 14214:2003) as shown in Table 2. Also, comparing the properties with the petroleum diesel is necessary for determining the validity of the biodiesel.

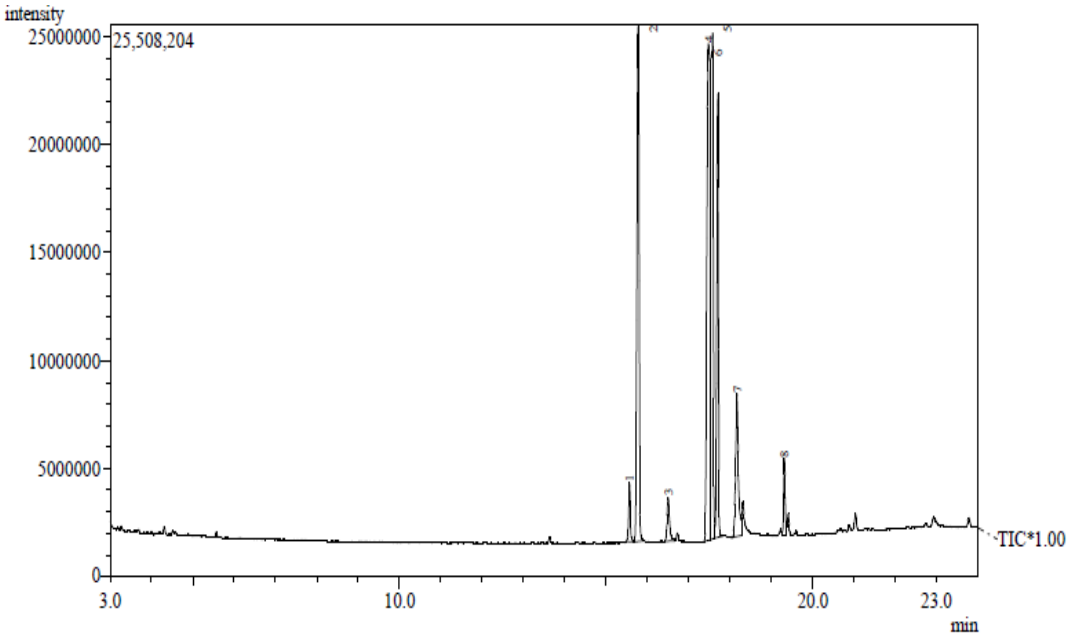

Fig. 1. GCMS Spectra of WCO showing peaks at different time intervals

Table 2. Fatty acid profile of WCO

Peaks	R Time	Compound	Area (%)
1	15.570	C19H36O2 Methyl (11E)-11-octadecenoic acid	1.67
2	15.790	C17H34O2 Methyl 14-methylpentadecanoic acid	21.50
3	16.511	C16H32O2 1-Pentadecanecarboxylic acid	1.91
4	17.486	C18H31ClO (9E,12E)-9,12-Octadecadienoyl chloride	26.43
5	17.583	C19H36O2 (E)-9-Octadecenoic acid methyl ester	26.20
6	17.710	C21H42O2 Methyl-aracidate or Methyl-eicosenate	12.92
7	18.176	C18H34O2 cis-9-Octadecenoic acid	7.20
8	19.320	C19H36O3 Methyl ricinolate	2.26

3.2 WTFS Characterization and Elemental Analysis

Fig. 2 shows the FT-IR spectra analysis of the WTFS catalyst calcined at 900 oC for 2 hours after pre-treatment. The absorbance bands match the WTFS vibrations during infra-red exposure. Table 3 gives the functional groups in the WTFS catalyst according to the spectrum stretching.

The XRD pattern of WTFS catalyst reflects the properties of a crystalline material with a single intense and sharp basal plane peak at low 2θ, a medium duplet, and a basal plane peak at high 2θ. All of the reflections are crisp, indicating that the material is extremely crystalline and contains few impurities. The XRF analysis gives the elemental composition confirmed by the XRD in Fig. 3. It shows a high concentration of CaO of 57.104 wt%, MgO of 21.195 wt%, Al_2O_3 of 13.949 wt%. This shows that the WTFS catalysts is comprised mainly of CaO, MgO and Al_2O_3. The other metal oxides present in the catalyst include PdO of 4.203 wt% while others are very low and has insignificant effect on the properties of the catalyst. These transition metals and their compounds are used as catalyst because of their ability to change oxidation state or in the case of the metals, to adsorb other substances on their surface as catalyst.

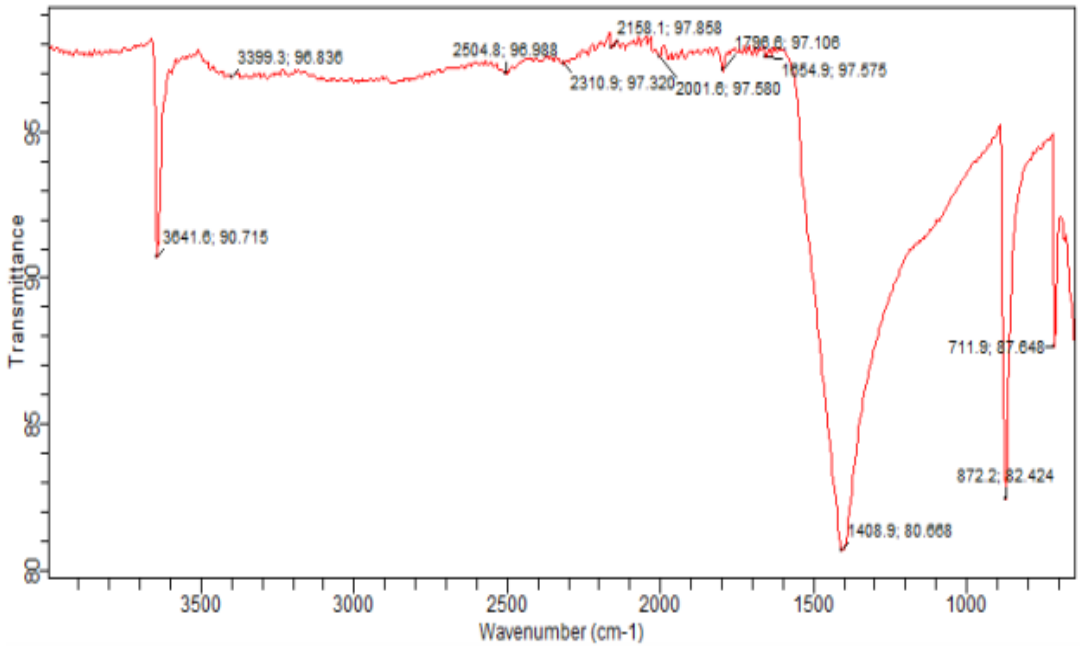

Fig. 2. FT-IR spectra of the WTFS catalyst

Table 3. Functional groups of WTFS catalyst

S/No.	Frequency (cm^{-1})	Appearance	Bonds	Compounds
1.	3641.6	Very sharp and weak absorption band	O-H stretching vibration (free)	Alcohols, phenol, water, ROH, ArOH, H_2O
2.	1408.9	Very sharp and broad absorption band	C-O stretching vibration of carbonate ion	CO3-, CO_2, CO
3.	872.2	Very sharp and broad absorption band	C-H bending vibration	RCH=CR, or mono substituted Arene ring
4.	711.9	Very sharp and broad absorption band	M-O stretching vibration	Ca – O, Mg – O, Al – O etc.

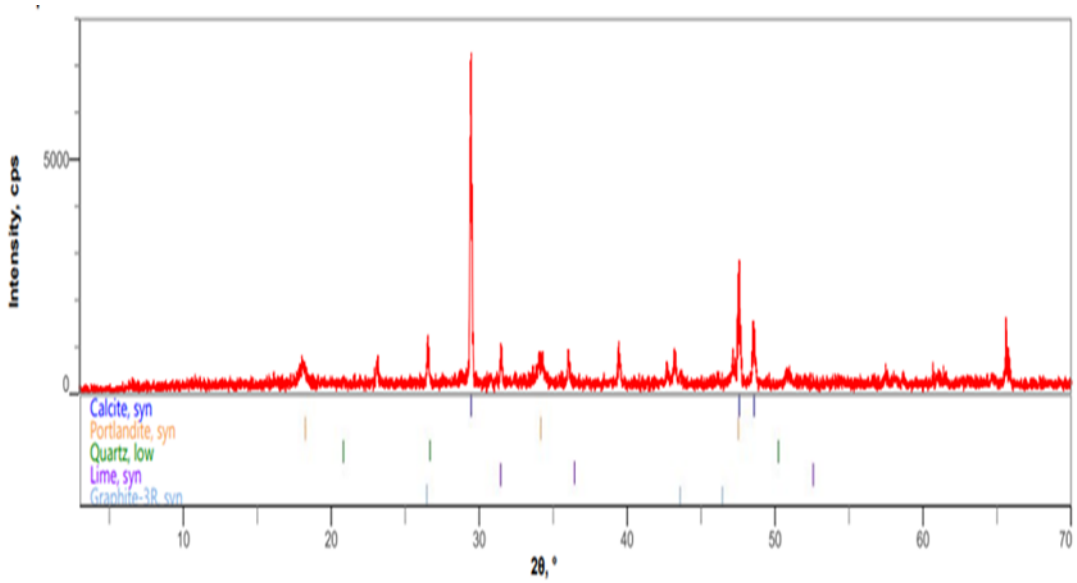

Fig. 3. X-ray diffraction of WTFS catalyst

3.3 Transesterification Reaction of WCO

3.3.1 Numerical optimization of reaction conditions for WCO to biodiesel using WTFS

The numerical optimization of the transesterification of WCO was carried out with the use of design expert software 8P using response surface methodology. Central Composite Design (CCD) was recommended by the software beased on the three-factors, three-level design. The quadratic model was chosen, the build time was 10 minutes and the subtype, randomoized to generate 20 runs as presented in Table 4. From the table, the highest biodiesel yield was 86.95% at the following conditions; 60^{o}C temperature, 5.50 wt.% catalyst loading, 105 minutes, and a constand methanol – oil ratio of 7:1. These results were analyzed numerically and Table 5 was gotten.

The Model F-value of 46.33 implies the model is significant. This means that there is only a 0.01% chance that a "Model F-Value" this large could occur due to noise. Based on the analysis of variance (ANOVA), the “p-value” value determined for the quadratic model was less than 0.05, suggesting that the design factors was significant. This means that the temperature (Factor A; p-value is < 0.0001), catalyst load (Factor B; p-value is 0.00713), time (factor C; p-value is 0.0288) and various interactions like;

- Interactions between the catalyst load and time (factor BC; p-value is < 0.0001)
- Quadratic factors; square of the temperatures (Factor A^2; p-value is < 0.0001), catalyst load squared (Factor B^2; p-value is 0.0016) and time squared (Factor C^2; p-value is 0.007).

Furthermore, to demonstrate the connection between biodiesel yield and the three significant factors, the interaction and the quadratic factors, the quadratic equation for the regression model in Equation (3) below is used:

$$Yield = 82.61 - 9.17A - 1.55B + 2.82C - 2.54AB + 1.64AC + 14.50BC - 16.11A^2 - 4.61B^2 - 3.64C^2 \quad (3)$$

Since the “Lact-of-Fit F-value” is 2.52, thus means that there is a 16.62% chance that the model would not fit the experiment thereby proving the suitablility of quadratic model for the experimental design.

The value of the coefficient of determination, often known as R^2, is a statistical metric that indicates the fraction of a dependent variable's variance that can be attributed to an independent variable or variables. The R^2 value provides a measure of how variability in the observed response values could be explained by the experimental factors and their interactions [63]. The R-squared (R^2) value was 0.9766 for methyl-ester (biodiesel) yield. The closer the R^2 value to 1, stronger the model and better it predicts the response. Therefore the R^2 value of 0.9766 showed that only about 2.34% of the total variation in the observed response

Table 4. RSM experimental design matrix and results of produced biodiesel

Standard order	Coded factors			Actual factors			Yield (%)	
	A	B	C	Temp (^oC)	Catalyst dosage (wt.%)	Time (mins)	Experimental	Predicted
1	-1	-1	-1	42.16	2.82	60.40	77.56	79.75
2	1	-1	-1	77.84	2.82	60.40	65.12	63.19
3	-1	1	-1	42.16	8.18	60.40	57.47	52.73
4	1	1	-1	77.84	8.18	60.40	22.70	26.02
5	-1	-1	1	42.16	2.82	149.60	58.22	53.10
6	1	-1	1	77.84	2.82	149.60	40.18	43.12
7	-1	1	1	42.16	8.18	149.60	83.96	82.61
8	1	1	1	77.84	8.18	149.60	67.93	63.94
9	-1.68	0	0	30.00	5.50	105.00	48.84	52.46
10	1.68	0	0	90.00	5.50	105.00	22.67	21.60
11	0	-1.68	0	60.00	1.00	105.00	71.90	72.17
12	0	1.68	0	60.00	10.00	105.00	64.68	66.96
13	0	0	-1.68	60.00	5.50	30.00	67.75	67.57
14	0	0	1.68	60.00	5.50	180.00	74.34	77.06
15	0	0	0	60.00	5.50	105.00	81.75	84.09
16	0	0	0	60.00	5.50	105.00	80.16	84.09
17	0	0	0	60.00	5.50	105.00	82.18	84.09
18	0	0	0	60.00	5.50	105.00	85.81	84.09
9	0	0	0	60.00	5.50	105.00	79.23	84.09
20	0	0	0	60.00	5.50	105.00	86.95	84.09

.

Table 5. ANOVA results for the quadratic response surface regression model

Source	Sum of Squares	Df	Mean Square	F-Value	p-value Prob > F
Model	6966.331	9	774.0368	46.33446	< 0.0001*
A-Temperature	1149.475	1	1149.475	68.8085	< 0.0001*
B-Catalyst Load	3279.335	1	3279.335	9.63033	0.00713*
C-Time	108.665	1	108.665	6.504776	0.0288*
AB	51.6128	1	51.6128	3.089583	0.1093
AC	21.58245	1	21.58245	1.291943	0.2822
BC	1682	1	1682	100.6859	< 0.0001*
A^2	3742.421	1	3742.421	224.0243	< 0.0001*
B^2	306.5278	1	306.5278	18.349	0.0016
C^2	190.7235	1	190.7235	11.41686	0.0070
Residual	167.0542	10	16.70542		
Lack of Fit	119.6566	5	23.93133	2.52453	0.1662
Pure Error	47.3976	5	9.47952		
Cor Total	7133.385	19			
Fit Statistics					
R^2 (%)	97.66				
Adjusted R^2 (%)	95.00				
Predicted R^2 (%)	84.68				
Coefficient of Variation	06.20				
Adequate Precision	21.00				

** means significant factors*

cannot be explained by this model. In addition, the regression coefficient (R^2) value of the actual experimental data (95%) and the predicted data (84.68%) result are obviously in resonance seeing that both values only differ by less than 11% and the coefficient of variance (error percentage) i.e. CV = 6.20% further proves that the model is a good fit. Similarly, the adequate precision of the model bothers around 21 which is largerly greater than "4" (the minimum limit) because a signal to noise ratio of greater than 4 is desirable to indicate that the model is suitable for navigating the design space.

The consistency plotting (Fig. 4) demonstrates a significant correlation between the actual and expected values of biodiesel production. The points concentrated around the diagonal line indicating a successful fit of the model with an insignificant residual value due to the low variance between the actual and forecast values. The impacts of interaction process variables on biodiesel yield were graphically explored using three-dimensional surface plots and two-dimensional contour plots. The biodiesel production is projected to grow at optimal values but decline if the values are increased past the optimum [49]. Figure 4a and 4b shows the interaction of recaction time and catalyst loading on the biodiesel yield. It can be seen that the yield of biodiesel increases with increase in reaction time towards 105 minutes up to 5.5 wt.% WTFS catalyst at a reaction temperature of 60 ^{o}C and after that, a steady fall in the yield with increase in the amount of WTFS catalyst and reaction time. The shape of contour plot revealed that more than 80% of biodiesel yield peaked between 2.82 and about 5.5 wt.% WTFS catalyst and 60 – 105 minutes' reaction time. However, there is a reduction in yield with longer time spent and larger amount of WTFS catalyst. This may be because of presence of excess catalyst which will in turn, make the separation of products very difficult by which the amount of catalyst must be optimized [64]. Adequate time is required for reactants to interact together to form product(s) [65]. Based on the results, it can be deduced that the reaction time and WTFS catalyst load play an important role in the biodiesel yield. Figs. 4c and 4d demonstrates the effects of varied reaction temperatures and amounts of additional WTFS catalyst on biodiesel yield while the reaction duration was held constant at 105 minutes. Increase in reaction temperature had a substantial effect on biodiesel yield under all conditions. With a minute change in biodiesel yield due to the catalyst load, biodiesel yield rose according to the reaction temperature. However, yield decreases significantly with increasing temperature

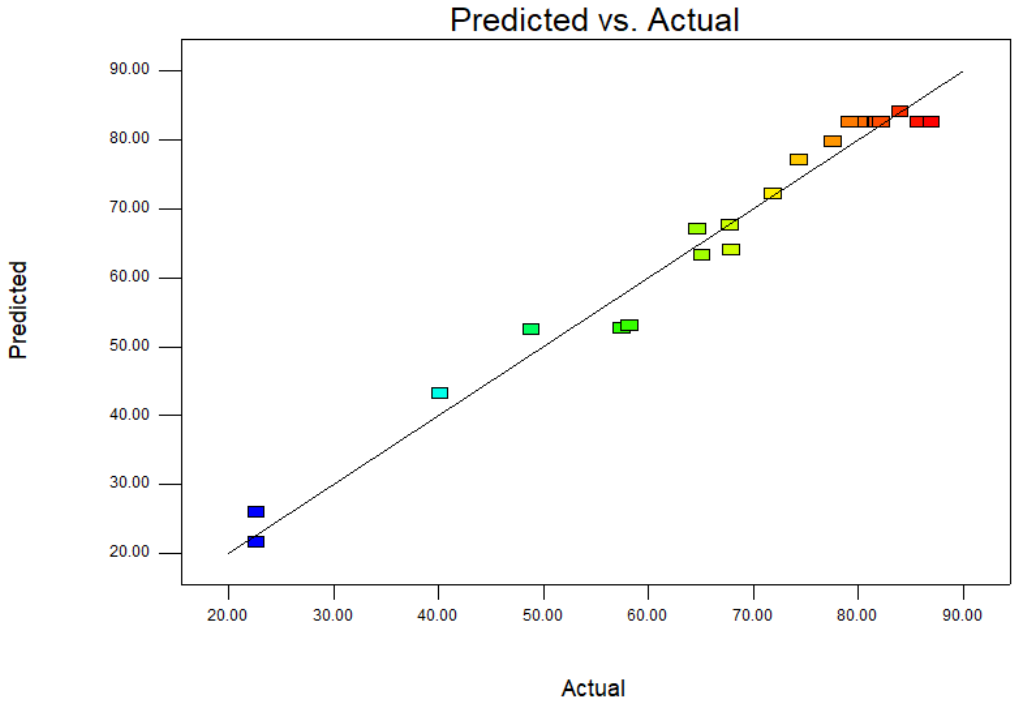

Fig. 4. Parity plot of biodiesel yield produced via WFTS catalysts

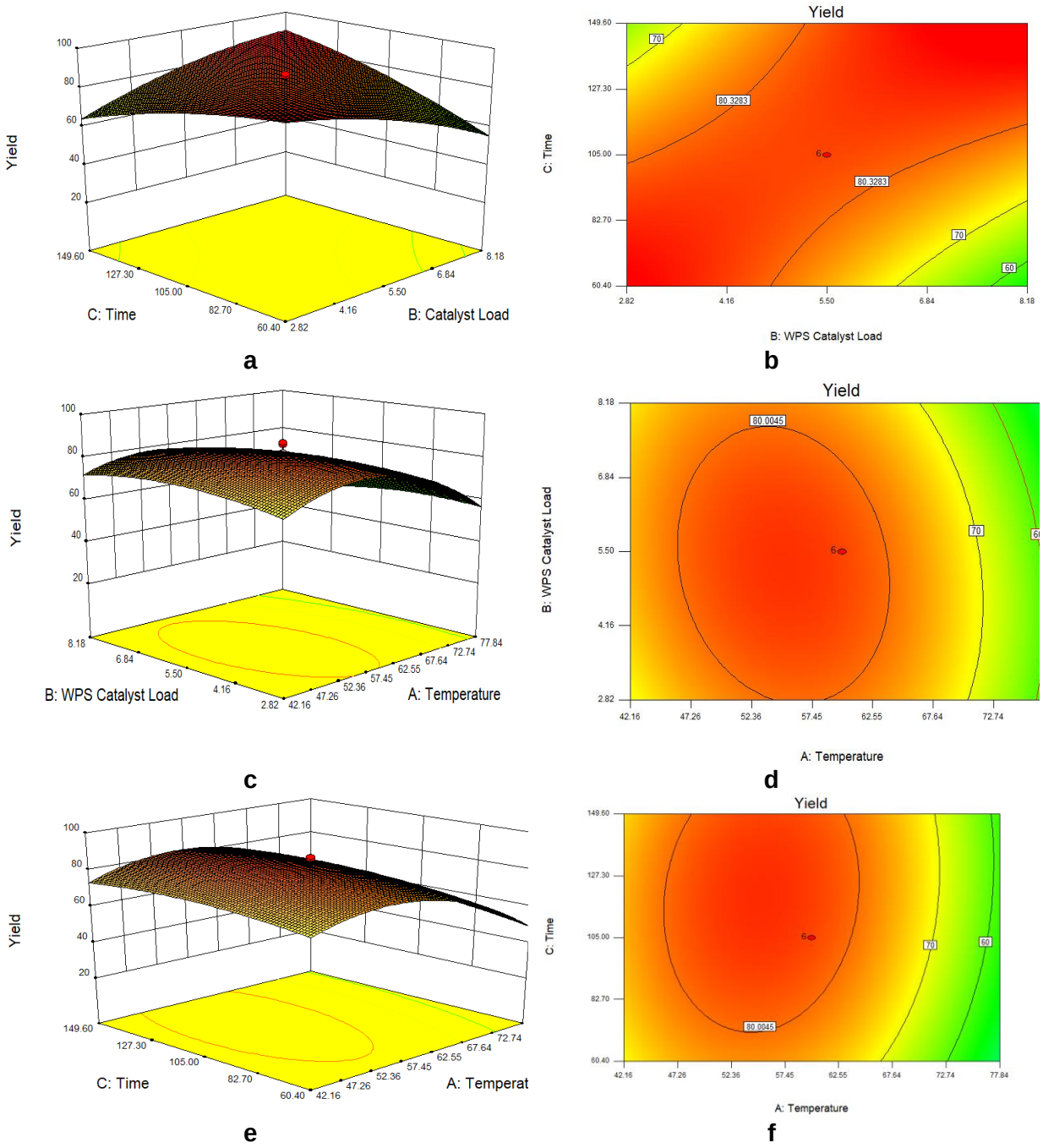

Fig. 5(a–f). 3-D Response Surface and contour plots for the interaction effects of process parameters

and WTFS catalyst concentration. This may be due to the boiling point of methanol (65^{o}C), which renders it unavailable for reaction [66]. In contrast, raising the designated amount of catalyst had a modest effect on the biodiesel output at different reaction temperatures. The maximum biodiesel was produced by employing a WTFS catalyst of roughly 5.5% by weight and 60^{o}C. Fig/ 4e and 4f illustrates the three-dimensional and contour response surface built to demonstrate the impact of the transesterification condition factors (temperature and reaction time) on biodiesel yield. The yield of biodiesel increases as the reaction temperature approaches 60^{o}C and the reaction time approaches 105 minutes with a WTFS catalyst loading of 5.5% by weight. Approximately in the vicinity of the optimal time and temperature, the

maximum yield was achieved. However, the reaction time has a more consistent effect on biodiesel yield than reaction temperature, as temperatures above 65°C resulted in a significant decrease in biodiesel yield at various reaction durations. Based on the data, it might be concluded that the reaction temperature had a greater impact on the biodiesel yield than the reaction time.

The density of the prepared biodiesel from WCO was found to be 5.30% higher than the average petrol diesel (0.8325 kg/m^3) as seen in Table 6. This is confirmed because the (average) densities of over 30 investigated methyl esters from different bio-sources and over 18 works, ranged from 0.75 to 0.904 kg/m^3, with the overall average value being 0.8802 kg/m^3 (i.e. almost 5% higher than the corresponding fossil diesel value) [18], [72]–[77]. Density can impact fuel consumption as fuel introduced into the combustion chamber is determined volumetrically [78]. Biodiesel fuels are, in general, characterized by higher density than conventional fossil diesel, which means that volumetrically operating fuel pumps will inject greater mass of biodiesel than fossil diesel fuel [79]. Since the flow is controlled by volume, the expected peak power reduction for engines using B100 is only 5 to 7% less than the fossil diesel because more (kg/m^3) would flow and vaporize more efficiently given a set throttle (volume) [80]. It should be noted that biodiesel produces more than three times the energy as the same amount of fossil fuel. Biodiesel's higher Specific gravity and density relative to fossil diesel means that on road biodiesel blends are normally made by splash blending the biodiesel fuel on top of the conventional diesel fuel or fossil fuel [80].

Kinematic viscosity is the primary reason why biodiesel is used as an alternative fuel instead of neat vegetable oils or animal fats [81]. The viscosity of the prepared biodiesel indicates a 65.187% decrease from the crude WCO. It is noticed that prepared biodiesel is 3.07% higher in value than the maximum allowable viscosity for a petroleum-derived diesel. The viscosity range given as per the ASTM D7042 and EN14214 standard is 1.9 to 6.0 mm^2/s [67], [68]. This high value is due to high fatty acid composition of the source oil (WCO in this case) [82]. Fatty acid composition determines the degree of saturation and the higher the composition the higher the degree of saturation. Viscosity increases with increasing degree of saturation [69].

The produced biodiesel has a higher flash point than that of petroleum diesel (104 ^{o}C > 55 ^{o}C minimum) because biodiesel has a higher number of fatty acid methyl esters (FAME) which is generally not volatile. Flash point varies inversely with the fuel's volatility hence; biodiesel is safer to handle at higher temperature than fossil diesel. As diesel impurities increase in biodiesel and diesel-fuel blends, so does the flash point increase [78]. Flow properties such as pour point (PP) and cloud point (CP) are important in determining performance of fuel flow system [69]. Viscosity is known to be inversely proportional to temperature,

Table 6. Quality of WCO, Biodiesel with EU and American Standards [67]–[71]

Property	WCO	Biodiesel (Prepared)	Biodiesel (EU & American Standards)	Petroleum Biodiesel
Relative density (15^{0}C) kg/m^3	909.8	880	860 – 900	832.5
Kinematic Viscosity (at 40^{0}C), mm^2/s	13.30	4.638	1.9 – 6.0	2.0 – 4.5
Acid value (mg KOH/g)	10.02	0.416	0.50 max	0.15
Peroxide value (meq/kg)	461.54	-	-	-
Iodine value (I_2/100g)	2167.87	92.57	120 max	-
Saponification value (mg KOH/g)	184.25	-	-	-
Ester value (mg KOH/g)	174.25	103.57	96.5 min	-
Free fatty acid content (%)	5.035	0.209	0.251 max	-
Percentage glycerol	9.53		0.240 max	-
Pour point (^{o}C)	5.2	0.3	0	1
Flash point (^{o}C)	156	104	120 – 130 min	55 min
Carbon-content (% m/m)	2.65	0.019	0.05 – 0.30 max	0.30 max
Cloud point (^{o}C)	10	1.3	No Report	2
Calorific value (MJ/kg)	34.78	40.17	25.35 – 43.96	44 – 46

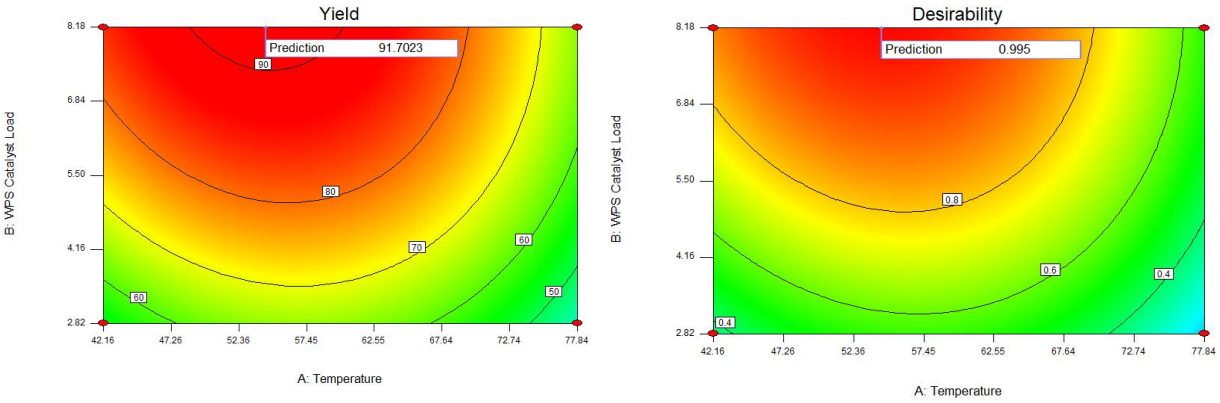

Fig. 6(a & b). Contour plot of optimized biodiesel yield and desirability

therefore, operating a diesel engine at low temperatures especially in cold climate regions can be difficult because of high viscosities.

The acid value for the prepared biodiesel from WCO (0.416) was about 67% higher than petroleum diesel (0.15) but falls within the required American and European standard for biodiesel. However, this is an indication that the biodiesel is more unstable compared with petroleum diesel [69]. The calorific value increased by 15.5% from its source waste cooking oil but 13% lower than petroleum-diesel calorific values.

3.3.2 Optimization of biodiesel yield

Using the Design of Expert 8P software, biodiesel yield was numerically optimise by first optimzing all factors and response variables. Since maximum biodiesel yield is desired, set the lower (30.67%) and upper ranges (92%). Table 4 codes independent variables as 1 and +1. Within the range, numerical optimization is performed. Based on the model and input criteria, the CCD provided the best system response optimizing biodiesel yield based on transesterification factors in experimental runs. The software projected that optimal parameters for biodiesel yield were 60°C temperature, 5.5 wt.% WTFS catalyst load, and 105 minutes of reaction time, with 86.95 percent biodiesel yield. After optimization the biodiesel production was 91.7%. This signifies that the experimental value agreed with the model's value.

4. CONCLUSION

The investigation on using waste *Tympanotonus fuscatus* shell (WTFS) as a catalyst in transesterifying high FFA waste cooking oil (WCO) led to the following conclusions:

i. Waste cooking oil (WCO) had a large amount of free fatty acid (FFA > 5%), thus direct transesterification couldn't be done. Initial esterification decreased the FFA to 1%.

ii. Using design expert 8P's central composite design (CCD) of response surface methodology (RSM), the subsequent transesterification process successfully optimised biodiesel yield (91.7%). Experiment design favoured the quadratic model. The three operating paramenters were significant from the ANOVA results (< 0.05 p-values) showing that the prepared catalyst had an influence on the biodiesel yield.Only the interaction variable of catalyst load and time was significant while all quadratic variables showed significance.

iii. The optimal reaction conditions were 60 ^{o}C, 5.5 wt. percent WTFS catalyst loading, and 105 minutes at a 7:1 methanol-oil ratio. Biodiesel yields were 86.75 percent anticipated and 91.70 percent optimised.

iv. X-ray diffraction and FTIR characterisation of WTFS showed the catalyst had a high percentage of CaO along with Al_2O_3, SiO_2, MgO, and traces of other metallic oxides, indicating WTFS is a promising catalyst source.

v. Gas chromatogram – mass spectroscopy (GCMS) analysis of improved biodiesel showed the presence of C16:0 (palmitic acid), C17:0 (methyl heptadecanoate), C18:1 (oleic acid), C18:2 (linoleic acid), and C18:3 derivatives (linolenic acid). The

physicochemical characterisation indicated similar qualities to American and European biodiesel, making it appropriate for blends and unblended application.

HIGHLIGHTS

- The waste cooking oil (WCO) was characterized with a high acid value content (10.02 mgKOH/g) and esterified to give an acid value of 0.416 (mgKOH/g).
- An effective catalyst used for the conversion of waste cooking oil to biodiesel was calcined at 900^{o}C for 2 hours.
- The central composite design (CCD) method for optimization was carried out using the three-level, three-factors factorial.
- Maximum validated biodiesel yield of 91.70 (%wt.) was obtained via numerical optimization.
- The produced biodiesel quality agrees with biodiesel standard.

FUNDING

This work receives no fund from any University, Private organization or Government body.

COMPETING INTERESTS

Authors have declared that no competing interests exist.

REFERENCES

1. Mercy Nisha Pauline JM, Sivaramakrishnan R, Pugazhendhi A, Anbarasan T, Achary A. Transesterification kinetics of waste cooking oil and its diesel engine performance. Fuel. Feb 2021;285:119108.
DOI: 10.1016/j.fuel.2020.119108.
2. Yusuff AS, Gbadamosi AO, Popoola LT. Biodiesel production from transesterified waste cooking oil by zinc-modified anthill catalyst: Parametric optimization and biodiesel properties improvement. J Environ Chem Eng. Apr 2021;9(2): 104955.
DOI: 10.1016/j.jece.2020.104955.
3. Santana JCC, Miranda AC, Souza L, Yamamura CLK, Coelho DdF, Tambourgi EB et al. Clean production of biofuel from waste cooking oil to reduce emissions, fuel cost, and respiratory disease hospitalizations. Sustainability. Aug 2021; 13(16):9185.
DOI: 10.3390/su13169185.
4. Kuniyil M, Shanmukha Kumar JV, Adil SF, Assal ME, Shaik MR, Khan M et al. Production of biodiesel from waste cooking oil using ZnCuO/N-doped graphene nanocomposite as an efficient heterogeneous catalyst. Arab J Chem. Mar 2021;14(3):102982.
DOI: 10.1016/j.arabjc.2020.102982.
5. Azman NS, Marliza TS, Mijan NA, Yun Hin TYY, Khairuddin N. Production of biodiesel from waste cooking oil via deoxygenation using Ni-Mo/Ac catalyst. Processes. 2021;9(5):12.
DOI: 10.3390/pr9050750.
6. Erchamo YS, Mamo TT, Workneh GA, Mekonnen YS. Improved biodiesel production from waste cooking oil with mixed methanol–ethanol using enhanced eggshell-derived CaO nano-catalyst. Sci Rep. 2021;11(1):6708.
DOI: 10.1038/s41598-021-86062-z, PMID 33758293.
7. Nadeem F, Bhatti IA, Ashar A, Yousaf M, Iqbal M, Mohsin M et al. Eco-benign biodiesel production from waste cooking oil using eggshell derived MM-CaO catalyst and condition optimization using RSM approach. Arabian Journal of Chemistry. 2021;14(8):11.
DOI: 10.1016/j.arabjc.2021.103263.
8. Katekaew S, Suiuay C, Senawong K, Seithtanabutara V, Intravised K, Laloon K. Optimization of performance and exhaust emissions of single-cylinder diesel engines fueled by blending diesel-like fuel from Yang-hard resin with waste cooking oil biodiesel via response surface methodology. Fuel. 2021;304: 12.
DOI: 10.1016/j.fuel.2021.121434.
9. Liu Y, Yang X, Adamu A, Zhu Z. Economic evaluation and production process simulation of biodiesel production from waste cooking oil. Current Research in Green and Sustainable Chemistry. 2021;4:55.
DOI: 10.1016/j.crgsc.2021.100091.
10. Naeem MM, Al-Sakkari EG, Boffito DC, Gadalla MA, Ashour FH. One-pot conversion of highly acidic waste cooking oil into biodiesel over a novel bio-based bi-

functional catalyst. Fuel. Jan 2021;283:118914.
DOI: 10.1016/j.fuel.2020.118914.

11. Tan YH, Abdullah MO, Nolasco-Hipolito C, Taufiq-Yap YH. Waste ostrich- and chicken-eggshells as heterogeneous base catalyst for biodiesel production from used cooking oil: Catalyst characterization and biodiesel yield performance. Appl Energy. Dec 2015;160:58-70.
DOI: 10.1016/j.apenergy.2015.09.023.
12. Rezania S, Oryani B, Park J, Hashemi B, Yadav KK, Kwon EE et al. Review on transesterification of non-edible sources for biodiesel production with a focus on economic aspects, fuel properties and by-product applications. Energy Convers Manag. Dec 2019;201:112155.
DOI: 10.1016/j.enconman.2019.112155.
13. Moyo LB, Iyuke SE, Muvhiiwa RF, Simate GS, Hlabangana N. Application of response surface methodology for optimization of biodiesel production parameters from waste cooking oil using a membrane reactor. S Afr J Chem Eng. 2021;35:1-7.
DOI: 10.1016/j.sajce.2020.10.002.
14. Arrais Gonçalves M, Karine Lourenço Mares E, Roberto Zamian J, Narciso da Rocha Filho G, Rafael Vieira da Conceição L. Statistical optimization of biodiesel production from waste cooking oil using magnetic acid heterogeneous catalyst MoO3/SrFe2O4. Fuel. Nov 2021;304:121463.
DOI: 10.1016/j.fuel.2021.121463.
15. Maegala NM, Anupriya S, Hazeeq Hazwan A, Nor Suhaila Y, Hasdianty A. Conversion of waste cooking oil to glycerol by halal microbial lipase. IOP Conf Ser Earth Environ Sci. Jul 2020;505(1): 012056.
DOI: 10.1088/1755-1315/505/1/012056.
16. Loizides M, Loizidou X, Orthodoxou D, Petsa D. Circular Bioeconomy in Action: Collection and Recycling of Domestic Used Cooking Oil through a Social, Reverse Logistics System. Recycling. Apr 2019;4(2):16.
DOI: 10.3390/recycling4020016.
17. Bhatia SK, Gurav R, Choi TR, Kim HJ, Yang SY, Song HS et al. Conversion of waste cooking oil into biodiesel using heterogenous catalyst derived from cork biochar. Bioresour Technol. Apr 2020; 302:122872.
DOI:10.1016/j.biortech.2020.122872, PMID 32014731.
18. Bukkarapu KR. Comparative study of different biodiesel–diesel blends. Int J Ambient Energy. Apr 2019;40(3):295-303.
DOI: 10.1080/01430750.2017.1393775.
19. Singh-Ackbarali D, Maharaj R, Mohamed N, Ramjattan-Harry V. Potential of used frying oil in paving material: solution to environmental pollution problem. Environ Sci Pollut Res Int. May 2017;24(13):12220-6.
DOI: 10.1007/s11356-017-8793-z, PMID 28353106.
20. Borges ME, Díaz L. Recent developments on heterogeneous catalysts for biodiesel production by oil esterification and transesterification reactions: a review. Renew Sustain Energy Rev. Jun 2012;16(5):2839-49.
DOI: 10.1016/j.rser.2012.01.071.
21. Helmi M, Tahvildari K, Hemmati A, Aberoomand azar P, Safekordi A. Phosphomolybdic acid/graphene oxide as novel green catalyst using for biodiesel production from waste cooking oil via electrolysis method: Optimization using with response surface methodology (RSM). Fuel. 2021;287:16.
DOI: 10.1016/j.fuel.2020.119528.
22. Okonkwo CP, Ajiwe VIE, Mmaduakor EC, Nwankwo NV. Modelling and Optimization of biodiesel Production Process Parameters from Jansa Seed Oil (*Cussonia bateri*) Using Artificial Neural Network. Am J Appl Chem; 2008.
23. Gouran A, Aghel B, Nasirmanesh F. Biodiesel production from waste cooking oil using wheat bran ash as a sustainable biomass. Fuel. 2021;295:9.
DOI: 10.1016/j.fuel.2021.120542.
24. Farooq M, Ramli A, Naeem A. Biodiesel production from low FFA waste cooking oil using heterogeneous catalyst derived from chicken bones. Renew Energy. Apr 2015;76:362-8.
DOI: 10.1016/j.renene.2014.11.042.
25. Farooq M, Ramli A, Naeem A, Mahmood T, Ahmad S, Humayun M et al. Biodiesel production from date seed oil (*Phoenix dactylifera* L.) via egg shell derived heterogeneous catalyst. Chemical Engineering Research and Design. 2018;132:644-51.
DOI: 10.1016/J.CHERD.2018.02.002.
26. Akhabue CE, Osa-Benedict EO, Oyedoh EA, Otoikhian SK. Development of a bio-

based bifunctional catalyst for simultaneous esterification and transesterification of neem seed oil: Modeling and optimization studies. Renew Energy. Jun 2020;152:724-35.
DOI: 10.1016/j.renene.2020.01.103.

27. Uprety BK, Chaiwong W, Ewelike C, Rakshit SK. Biodiesel production using heterogeneous catalysts including wood ash and the importance of enhancing byproduct glycerol purity. Energy Convers Manag. May 2016;115:191-9.
DOI: 10.1016/j.enconman.2016.02.032.
28. Ezebor F, Khairuddean M, Abdullah AZ, Boey PL. Oil palm trunk and sugarcane bagasse derived heterogeneous acid catalysts for production of fatty acid methyl esters. Energy. 2014;70(C):493-503.
DOI: 10.1016/j.energy.2014.04.024.
29. Ho WWS, Ng HK, Gan S. Development and characterisation of novel heterogeneous palm oil mill boiler ash-based catalysts for biodiesel production. Bioresour Technol. Dec 2012;125:158-64.
DOI:10.1016/j.biortech.2012.08.099, PMID 23026328.
30. Endut A, Abdullah SHYS, Hanapi NHM, Hamid SHA, Lananan F, Kamarudin MKA et al. Optimization of biodiesel production by solid acid catalyst derived from coconut shell via response surface methodology. Int Biodeterior Biodegrad. Oct 2017;124:250-7.
DOI: 10.1016/j.ibiod.2017.06.008.
31. Etim AO, Betiku E, Ajala SO, Olaniyi PJ, Ojumu TV. Potential of ripe plantain fruit peels as an ecofriendly catalyst for biodiesel synthesis: optimization by artificial neural network integrated with genetic algorithm. Sustainability. Mar 2018;10(3):Art no. 3.
DOI: 10.3390/su10030707.
32. Gohain M, Devi A, Deka D. Musa balbisiana Colla peel as highly effective renewable heterogeneous base catalyst for biodiesel production. Ind Crops Prod. 2017;109(Aug):8-18.
DOI: 10.1016/j.indcrop.2017.08.006.
33. Nisar J, Razaq R, Farooq M, Iqbal M, Khan RA, Sayed M et al. Enhanced biodiesel production from Jatropha oil using calcined waste animal bones as catalyst. Renew Energy. Feb 2017;101:111-9.
DOI: 10.1016/j.renene.2016.08.048.
34. Ranganathan SV, Narasimhan SL, Muthukumar K. An overview of enzymatic production of biodiesel. Bioresour Technol. Jul 2008;99(10):3975-81.
DOI: 10.1016/j.biortech.2007.04.060, PMID 17591439.
35. Gama PE, Gil RAdSS, Lachter ER. Produção de biodiesel através de transesterificação in situ de sementes de girassol via catálise homogênea e heterogênea. Quím Nova. 2010;33(9):1859-62.
DOI: 10.1590/S0100-40422010000900007.
36. Aimikhe VJ, Lekia GB. ”An Overview of the Applications of Periwinkle (Tympanotonus fuscatus) Shells”, CJAST. CJAST. Aug 2021:31-58.
DOI: 10.9734/cjast/2021/v40i1831442.
37. Mo KH, Alengaram UJ, Jumaat MZ, Lee SC, Goh WI, Yuen CW. Recycling of seashell waste in concrete: A review. Construction and Building Materials. 2018;162:751-64.
DOI: 10.1016/J.CONBUILDMAT.2017.12.009.
38. Hou Y, Shavandi A, Carne A, Bekhit AA, Ng TB, Cheung RCF et al. Marine shells: Potential opportunities for extraction of functional and health-promoting materials. Crit Rev Environ Sci Technol. 2016 [online];46(11-12):1047-116.
DOI: 10.1080/10643389.2016.1202669.
39. Piker A, Tabah B, Perkas N, Gedanken A. A green and low-cost room temperature biodiesel production method from waste oil using egg shells as catalyst. Fuel. Oct 2016;182:34-41.
DOI: 10.1016/j.fuel.2016.05.078.
40. Viriya-empikul N, Krasae P, Puttasawat B, Yoosuk B, Chollacoop N, Faungnawakij K. Waste shells of mollusk and egg as biodiesel production catalysts. Bioresour Technol. May 2010;101(10):3765-7.
DOI: 10.1016/j.biortech.2009.12.079, PMID 20079632.
41. Waste shells of mollusk and egg as biodiesel production catalysts – ScienceDirect [cited May 30, 2022].
Available:https://www.sciencedirect.com/science/article/abs/pii/S0960852409017441.
42. Kurniawan E, Perdana F. Biodiesel production of waste cooking oil catalyzed by CAO derived from snail (achatina FULICA) shell waste. J Chem Process Mater Technol. Jan 2022;1(1):Art no. 1.
DOI: 10.36499/jcpmt.v1i1.5860.
43. Phewphong S, Roschat W, Pholsupho P, Moonsin P, Promarak V, Yoosuk B.

Biodiesel production process catalyzed by acid-treated golden apple snail shells (Pomacea canaliculata)-derived CaO as a high-performance and green catalyst. Eng Appl Sci Res. 2022;49(1):Art no. 1.

44. Kaewdaeng S, Sintuya P, Nirunsin R. Biodiesel production using calcium oxide from river snail shell ash as catalyst. Energy Procedia. Oct 2017;138:937-42. DOI: 10.1016/j.egypro.2017.10.057.
45. Liu H, Guo Hs, Wang Xj, Jiang Jz, Lin H, Han S et al. Mixed and ground KBr-impregnated calcined snail shell and kaolin as solid base catalysts for biodiesel production. Renew Energy. Aug 2016;93:648-57. DOI: 10.1016/j.renene.2016.03.017.
46. Ogunsola AD, Durowoju MO, Alade AO, Jekayinfa SO, Ogunkunle O. Modeling and optimization of two-step shea butter oil biodiesel synthesis using snail shells as heterogeneous base catalysts. Energy Adv. 2022;1(2):113-28. DOI: 10.1039/D1YA00042J.
47. Optimization and kinetic study of biodiesel production from Hydnocarpus wightiana oil and dairy waste scum using snail shell CaO nanocatalyst – ScienceDirect [cited May 30, 2022]. Available:https://www.sciencedirect.com/science/article/abs/pii/S0960148119310018.
48. Laskar IB, Rajkumari K, Gupta R, Chatterjee S, Paul B, Rokhum SL. Waste snail shell derived heterogeneous catalyst for biodiesel production by the transesterification of soybean oil. RSC Adv. 2018;8(36):20131-42. DOI: 10.1039/C8RA02397B, PMID 35541639.
49. Silitonga AS, Shamsuddin AH, Mahlia TMI, Milano J, Kusumo F, Siswantoro J et al. Biodiesel synthesis from Ceiba pentandra oil by microwave irradiation-assisted transesterification: ELM modeling and optimization. Renew Energy. Feb 2020;146:1278-91. DOI: 10.1016/j.renene.2019.07.065.
50. Adepoju TF, Ibeh MA, Udoetuk EN, Babatunde EO. Quaternary blend of Carica papaya - Citrus sinesis - Hibiscus sabdariffa - Waste used oil for biodiesel synthesis using CaO-based catalyst derived from binary mix of Lattorina littorea and Mactra coralline shell. Renew Energy. Jun 2021;171:22-33. DOI: 10.1016/j.renene.2021.02.020.
51. Akpa JG, Dagde KK. Effect of activation method and agent on the characterization of Prewinkle shell activated carbon. Chem Process Eng Research. 2018;56(0):24.
52. Offiong UD, Akpan GE. Assessment of physico-chemical properties of periwinkle shell ash as partial replacement for cement in concrete. 2017;1(7):4.
53. Omar WNNW, Nordin N, Mohamed M, Amin NAS. A two-step biodiesel production from waste cooking oil: optimization of pre-treatment step. J Appl Sci. 2009;9(17):3098-103. DOI: 10.3923/jas.2009.3098.3103.
54. Sanli H, Canakci M. Effects of different alcohol and catalyst usage on biodiesel production from different vegetable oils. Energy Fuels. Jul 2008;22(4):2713-9. DOI: 10.1021/ef700720w.
55. Thangaraj B, Solomon PR, Muniyandi B, Ranganathan S, Lin L. Catalysis in biodiesel production—a review. Clean Energy. Feb 2019;3(1):2-23. DOI: 10.1093/ce/zky020.
56. Yan S, Kim M, Salley SO, Ng KYS. Oil transesterification over calcium oxides modified with lanthanum. Applied Catalysis A: General. 2009;360(2):163-70. DOI: 10.1016/J.APCATA.2009.03.015.
57. Keihani M, Esmaeili H, Rouhi P. ”Biodiesel Production from Chicken Fat Using Nano-calcium Oxide Catalyst and Improving the Fuel Properties via Blending with Diesel”, PCR. Vol. 6(3, Sep); 2018. DOI: 10.22036/pcr.2018.114565.1453.
58. Eryilmaz T. Process optimization for biodiesel production from neutralized waste cooking oil and the effect of this biodiesel on engine performance. CT&F Cienc Tecnol Futuro. Jun 2018;8(1):121-7. DOI: 10.29047/01225383.99.
59. Musa H, Eric D, Hassan A, Usman B, Isa NF, Alhassan AS. Optimized biodiesel Production from Jatropha curcas oil. Energy Res J. Jan 2021;12(1):39-44. DOI: 10.3844/erjsp.2021.39.44.
60. Fatima A, Zafar M, Ahmad M, Sultana S, Ali MI. ”Parametric characterization and statistical optimization of *Argemone ochroleuca* (Mexican Poppy) methyl esters as a renewable source of energy”, null. Energy Sources Part A: Recovery Utilization and Environmental Effects. Oct 2017;39(19):1963-9. DOI: 10.1080/15567036.2017.1391896.

61. Leung DYC, Guo Y. Transesterification of neat and used frying oil: Optimization for biodiesel production. Fuel Process Technol. Oct 2006;87(10):883-90. DOI: 10.1016/j.fuproc.2006.06.003.
62. Adepoju TF. Optimization processes of biodiesel production from pig and neem (Azadirachta indica a.Juss) seeds blend oil using alternative catalysts from waste biomass. Ind Crops Prod. Jul 2020;149:112334. DOI: 10.1016/j.indcrop.2020.112334.
63. Tang Y, Chen G, Zhang J, Lu Y. Highly active CaO for the transesterification to biodiesel production from rapeseed oil. Bull Chem Soc Eth. 2011;25(1):Art no. 1. DOI: 10.4314/bcse.v25i1.63359.
64. Trejo-Zárraga F, Hernández-Loyo Fde J, Chavarría-Hernández JC, Sotelo-Boyás R. Kinetics of transesterification processes for biodiesel production. IntechOpen; 2018. DOI: 10.5772/intechopen.75927.
65. Ogaga Ighose B, Adeleke IA, Damos M, Adeola Junaid H, Ernest Okpalaeke K, Betiku E. Optimization of biodiesel production from Thevetia peruviana seed oil by adaptive neuro-fuzzy inference system coupled with genetic algorithm and response surface methodology. Energy Conversion and Management. 2017 [online];132:231-40. DOI: 10.1016/j.enconman.2016.11.030.
66. Mansourpoor M. Optimization of biodiesel production from sunflower oil using response surface methodology. J Chem Eng Process Technol. 2012;03(5). DOI: 10.4172/2157-7048.1000141.
67. Barabas I, Todoru I-A. Biodiesel quality, standards and properties. In:Tech Montero G, editor, Biodiesel- quality, emissions and by-products; 2011. DOI: 10.5772/25370.
68. Montero G, Stoytcheva M. Biodiesel-quality, emissions and by-products; 2011.
69. Ayetor GK, Sunnu A, Parbey J. Effect of biodiesel production parameters on viscosity and yield of methyl esters: Jatropha curcas, Elaeis guineensis and Cocos nucifera. Alex Eng J. Dec 2015;54(4):1285-90. DOI: 10.1016/j.aej.2015.09.011.
70. EN 14214; Nov 07, 2021. Wikipedia, Wikipedia. [accessed: Jun 04, 2022] [online]. Available:https://en.wikipedia.org/w/index.php?title=EN_14214&oldid=1054080525.
71. Alternative fuels data center: ASTM biodiesel specifications [cited Jun 04, 2022]. Available:https://afdc.energy.gov/fuels/biodiesel_specifications.html.
72. Ramírez Verduzco LF. Density and viscosity of biodiesel as a function of temperature: Empirical models. Renew Sustain Energy Rev. Mar 2013;19:652-65. DOI: 10.1016/j.rser.2012.11.022.
73. Pratas MJ, Freitas S, Oliveira MB, Monteiro SC, Lima AS, Coutinho JAP. Densities and viscosities of minority fatty acid methyl and ethyl esters present in biodiesel. J Chem Eng Data. May 2011;56(5):2175-80. DOI: 10.1021/je1012235.
74. Giakoumis EG, Sarakatsanis CK. Estimation of biodiesel cetane number, density, kinematic viscosity and heating values from its fatty acid weight composition. Fuel. Jun 2018;222:574-85. DOI: 10.1016/j.fuel.2018.02.187.
75. Bencheikh K, Atabani AE, Shobana S, Mohammed MN, Uğuz G, Arpa O et al. Fuels properties, characterizations and engine and emission performance analyses of ternary waste cooking oil biodiesel–diesel–propanol blends. Sustain Energy Technol Assess. Oct 2019;35:321-34. DOI: 10.1016/j.seta.2019.08.007.
76. Gülüm M, Bilgin A. A comprehensive study on measurement and prediction of viscosity of biodiesel-diesel-alcohol ternary blends. Energy. Apr 2018;148:341-61. DOI: 10.1016/j.energy.2018.01.123.
77. Razzaq L, Farooq M, Mujtaba MA, Sher F, Farhan M, Hassan MT et al. Modeling viscosity and density of ethanol-diesel-biodiesel ternary blends for sustainable environment. Sustainability. 2020;12(12):5186. DOI: 10.3390/su12125186.
78. Hossain AK, Davies PA. Plant oils as fuels for compression ignition engines: A technical review and life-cycle analysis. Renew Energy. 2010;35(1):1-13. DOI: 10.1016/j.renene.2009.05.009.
79. Tesfa B, Mishra R, Gu F, Powles N. Prediction models for density and viscosity of biodiesel and their effects on fuel supply system in CI engines. Renew Energy. Dec 2010;35(12):2752-60. DOI: 10.1016/j.renene.2010.04.026.

80. Nabi MdN, Rahman MM, Akhter MS, Md. M. Rahman, and Md.S. Akhter. Appl Therm Eng. Aug 2009;29(11-12):2265-70. DOI:10.1016/j.applthermaleng.2008.11.009.
81. Moser B. Biodiesel production, properties, and feedstocks. In Vitro Cell Dev Biol Plant. 2010;45:285-347. DOI: 10.1007/978-1-4419-7145-6_15.
82. Roy MM, Wang W, Bujold J. Biodiesel production and comparison of emissions of a DI diesel engine fueled by biodiesel–diesel and canola oil–diesel blends at high idling operations. Appl Energy. 2013; 106(C):198-208. DOI: 10.1016/j.apenergy.2013.01.057.

Peer-review history:
The peer review history for this paper can be accessed here:
https://www.sdiarticle5.com/review-history/89970